Clinical Cancer Research

A Phase II Trial of the Aurora Kinase A Inhibitor Alisertib for Patients with Castration-resistant and Neuroendocrine Prostate Cancer: Efficacy and Biomarkers

Himisha Beltran[1,2], Clara Oromendia[3], Daniel C. Danila[4,5], Bruce Montgomery[6], Christopher Hoimes[7], Russell Z. Szmulewitz[8], Ulka Vaishampayan[9], Andrew J. Armstrong[10], Mark Stein[11], Jacek Pinski[12], Juan M. Mosquera[2,13], Verena Sailer[2], Rohan Bareja[2], Alessandro Romanel[14], Naveen Gumpeni[15], Andrea Sboner[2,13], Etienne Dardenne[13], Loredana Puca[1,2], Davide Prandi[14], Mark A. Rubin[2,13], Howard I. Scher[4,5], David S. Rickman[2,13], Francesca Demichelis[2,14], David M. Nanus[1,2], Karla V. Ballman[3], and Scott T. Tagawa[1,2]

Abstract

Purpose: Neuroendocrine prostate cancer (NEPC) is an aggressive variant of prostate cancer that may develop *de novo* or as a mechanism of treatment resistance. N-myc is capable of driving NEPC progression. Alisertib inhibits the interaction between N-myc and its stabilizing factor Aurora-A, inhibiting N-myc signaling, and suppressing tumor growth.

Patients and Methods: Sixty men were treated with alisertib 50 mg twice daily for 7 days every 21 days. Eligibility included metastatic prostate cancer and at least one: small-cell neuroendocrine morphology; ≥50% neuroendocrine marker expression; new liver metastases without PSA progression; or elevated serum neuroendocrine markers. The primary endpoint was 6-month radiographic progression-free survival (rPFS). Pretreatment biopsies were evaluated by whole exome and RNA-seq and patient-derived organoids were developed.

Results: Median PSA was 1.13 ng/mL (0.01–514.2), number of prior therapies was 3, and 68% had visceral metastases. Genomic alterations involved *RB1* (55%), *TP53* (46%), *PTEN* (29%), *BRCA2* (29%), and *AR* (27%), and there was a range of androgen receptor signaling and NEPC marker expression. Six-month rPFS was 13.4% and median overall survival was 9.5 months (7.3–13). Exceptional responders were identified, including complete resolution of liver metastases and prolonged stable disease, with tumors suggestive of N-myc and Aurora-A overactivity. Patient organoids exhibited concordant responses to alisertib and allowed for the dynamic testing of Aurora–N-myc complex disruption.

Conclusions: Although the study did not meet its primary endpoint, a subset of patients with advanced prostate cancer and molecular features supporting Aurora-A and N-myc activation achieved significant clinical benefit from single-agent alisertib.

Introduction

Prostate cancer arises as an androgen-driven disease, and systemic therapies targeting the androgen receptor (AR) are a mainstay of treatment for patients at all stages of the disease. Most tumors that develop resistance to AR therapies remain dependent on AR signaling through AR mutation, overexpression, or other means (1). However in recent years, with the earlier and more potent targeting of the AR with newer drugs, non-AR–driven prostate cancer has emerged as a clinically relevant problem

[1]Department of Medicine, Weill Cornell Medicine, New York, New York. [2]Englander Institute for Precision Medicine, New York Presbyterian Hospital- Weill Cornell Medicine, New York, New York. [3]Department of Biostatistics, Weill Cornell Medicine, New York, New York. [4]Department of Medicine, Memorial Sloan Kettering Cancer Center, New York, New York. [5]Weill Cornell Medical College, New York, New York. [6]Department of Medicine, University of Washington, Seattle, Washington. [7]Department of Medicine, Case Western Reserve University, Cleveland, Ohio. [8]Department of Medicine, University of Chicago, Chicago, Illinios. [9]Department of Oncology, Wayne State University/Karmanos Cancer Institute, Detroit, Michigan. [10]Departments of Medicine, Surgery, and Pharmacology and Cancer Biology, Duke Cancer Institute, Duke University, Durham, North California. [11]Division of Medical Oncology, Rutgers Cancer Institute of New Jersey and Rutgers Robert Wood Johnson Medical School, New Brunswick, New Jersey. [12]Division of Oncology, University of Southern California, Norris Comprehensive Cancer Center, Los Angeles, California. [13]Department of Pathology and Laboratory Medicine, Weill Cornell Medicine, New York, New York. [14]Centre for Integrative Biology (CIBIO), University of Trento, Trento Italy. [15]Department of Radiology, Weill Cornell Medicine, New York, New York.

Note: Supplementary data for this article are available at Clinical Cancer Research Online (http://clincancerres.aacrjournals.org/).

Clinical Trial ID: NCT01799278

Corresponding Author: Himisha Beltran, Weill Cornell Medicine, 525 East 68th Street, Box 403, New York, NY 10021. Phone: 646-962-2072; Fax: 646-962-1603; E-mail: hip9004@med.cornell.edu

doi: 10.1158/1078-0432.CCR-18-1912

Translational Relevance

A subset of prostate cancers evade androgen receptor (AR)-targeted therapies through the development of lineage plasticity, neuroendocrine features, and loss of AR signaling dependence, with prior translational data pointing to N-myc and Aurora kinase A as key targets. In this phase II trial, clinically enriched for patients with AR-independent and neuroendocrine prostate cancer (NEPC), we investigated the efficacy of alisertib, a drug that inhibits the allosteric interaction between N-myc and Aurora-A. Exceptional responders were identified and characterized, suggesting that some but not all patients with NEPC do benefit from alisertib. Pretreatment biopsies were performed in all patients to understand the clinical, pathologic, and molecular features underlying response to alisertib and to characterize the molecular characteristics of this aggressive subgroup of prostate cancer.

(2, 3). This has been associated with low AR signaling, loss of luminal prostate markers, and the development of small-cell neuroendocrine features through a process of lineage plasticity (3–6). Patients with AR-independent neuroendocrine prostate cancer (NEPC) often present with metastatic disease to visceral sites in the setting of a low or modestly rising serum PSA (7). NEPC may share morphologic, clinical, and molecular (e.g., *RB1* and *TP53* loss) features with small-cell carcinoma of the lung (8), and patients are often treated with similar platinum-based chemotherapy regimens (9–11). Prognosis is poor and new therapies are urgently needed (3, 12).

We previously identified the oncogenic transcriptional factor N-Myc and the cell-cycle kinase Aurora kinase A as overexpressed in the majority of metastatic neuroendocrine prostate tumors and a subset of castration-resistant prostate adenocarcinomas (CRPC-Adeno; ref. 13). N-myc is capable of suppressing AR signaling and driving lineage plasticity, tumor aggressiveness, and AR-independent progression in prostate cancer preclinical models (14, 15). Aurora-A stabilizes N-myc and prevents N-myc protein degradation in human neuroblastoma and in prostate cancer (13–16). The Aurora kinase A catalytic inhibitor alisertib also disrupts the N-myc–Aurora A protein complex (17), thereby inhibiting N-myc signaling and tumor growth.

In this study, we aimed to investigate the clinical efficacy of alisertib in patients with the NEPC phenotype. As NEPC is not well-defined clinically, we established distinct eligibility criteria to capture the range of clinical and pathologic definitions within the "NEPC syndrome" with shared biologic features. A mandatory pretreatment biopsy was performed in all patients to investigate the relationship between biopsy pathology and molecular features and clinical characteristics. Our objective of this trial was to identify the clinical characteristics and molecular profiles of responding patients to define distinct cohorts most likely to benefit.

Patients and Methods

In this single-arm, multi-institutional open-label phase II trial of the Department of Defense Prostate Cancer Clinical Trials Consortium (NCT01799278), patients with metastatic prostate cancer and at least one of the following key eligibility criteria were enrolled across 9 centers between 2013 and 2016: (i) small-cell NEPC morphology (determined by the enrolling center) on the basis of any current or prior tissue sample, (ii) prostate adenocarcinoma with greater than 50% IHC staining for neuroendocrine markers (e.g., chromogranin and synaptophysin), (iii) development of liver metastases in the absence of PSA progression defined by Prostate Cancer Working Group 2 criteria (18), and (iv) serum chromogranin A level $\geq 5\times$ upper limit of normal (ULN) and/or serum neuron specific enolase (NSE) $\geq 2\times$ ULN. Institutional review board approval was obtained (see trial protocol, Supplementary Data) and all patients gave written informed consent. The study was conducted in accordance with ethical principles founded in the Declaration of Helsinki.

A new metastatic pretreatment biopsy was sent centrally for pathology review and molecular analysis. Patients were treated with alisertib (Millennium Pharmaceuticals) at the recommended phase II dose of 50 mg twice daily for 7 days every 21 days and followed with radiographic evaluation every 3 cycles. Concomitant proton pump inhibitor medication was not allowed on study (see protocol, Supplementary Data). Dose reductions were specified on the basis of adverse events (AEs). Therapy was continued until disease progression, unacceptable toxicity, or withdrawal of consent. The primary endpoint was 6-month radiographic progression-free survival (rPFS). Secondary endpoints included response rate, overall survival (OS), and toxicity.

Whole-exome sequencing (WES) and RNA-seq analysis were performed using protocols described previously (4) with the addition of Excavator (19) for copy-number segmentation. Targeted mRNA gene expression (NanoString) was performed in cases without sufficient frozen tissue using a published assay (20). *AURKA* and *MYCN* dual-color FISH amplification was defined by the presence of ≥ 4 copies per nucleus with >100 nuclei evaluated per section (13, 21). Patient-derived organoids were developed from fresh tissues using published protocols (22, 23). Organoids were treated with alisertib and viability determined using CellTiter-Glo (Promega). A proximity ligation assay of N-Myc–Aurora A interaction was applied to human tissues using protocols described by Dardenne and colleagues (14).

Statistical analysis

On the basis of the phase II trial of danusertib (24), less than 15% of unselected patients with metastatic castration-resistant prostate cancer (CRPC) would be expected to respond to single-agent Aurora kinase inhibition. Radiographic response rate was initially selected as the primary endpoint. The trial was amended after an interim analysis of the first 19 patients demonstrating limited responses but with clinical improvement and stable disease in this patient population with aggressive disease and limited treatment options. On the basis of recommendations of the steering committee, the primary endpoint was modified to 6-month rPFS. This was an endpoint also used in other recent clinical studies including Rathkopf and colleagues (25). Secondary endpoints included response rate and OS. The null hypothesis (H0) was that $\leq 15\%$ of patients would be radiographic progression-free at 6 months and the alternative hypothesis (Ha) was $\geq 30\%$. A sample size of 48 patients was determined according to Ahern's exact single-stage phase II design (ref. 26; 5% significance, 80% power). Requiring at least 20% to have histologic entry criteria to assess sufficient patients with NEPC, we planned to treat a total 60 patients. All patients who received at least 1 dose of alisertib were included in the safety analysis. Toxicities were

graded according to CTCAEv.4.0. Analysis for organoid treatment was performed on 3 independent biological replicates using a nonlinear regression curve fit (3 parameters) method in Prism 6. All other analyses were performed in R 3.2.3.

Results

A total of 75 patients were screened and 60 patients were treated. At the end of the study, 48 patients (80%) had died, and median follow-up among patients not known to be deceased was 9.7 months (1.1–14.9). Median age was 67 years (45–87), median PSA 1.13 ng/mL (0.01–514.2; Table 1). Thirty-seven patients (61%) received prior local therapy for prostate cancer and the median number of prior systemic therapies was 3 (40% enzalutamide or abiraterone, 32% docetaxel, and 58% platinum chemotherapy). The majority of patients had adverse prognostic risk factors, including visceral metastases (68%) and elevated LDH (53%; median 233, 109–1,428). By central labs, serum neuroendocrine markers were elevated above the ULN in 46 of 55 (84%) evaluable patients (chromogranin 71%, NSE 47%; concordance 51%). Carcinoembryonic antigen (CEA) was elevated in 18 of 31 (58%) evaluable patients (median 18.1, 2.3–204.5).

Seventy-five percent (45) of treated patients had pathologic features of NEPC at screening. Of the others with adenocarcinoma, eligibility was based on IHC (5), serum neuroendocrine markers (6), and liver metastases without PSA progression (6). Overall, 35% (21) met more than one key eligibility criteria (Supplementary Table S1). All patients underwent a new pretreatment metastatic biopsy, of which 56 of 60 were evaluable by central review, and tumors were classified as NEPC on the basis of published morphologic criteria (27) or CRPC-Adeno. NEPC pathology concordance rate between study biopsy and screening tissue was 75% (42/56; Supplementary Table S1) with differences likely reflecting heterogeneity, temporal differences, and/or possibly interreader variability between centers. By central review, 54% of evaluable patients (30/56) were classified as NEPC on the basis of morphologic criteria (27); of these, 73% (22) were small-cell carcinoma, 23% (7) neuroendocrine differentiation, and one mixed small-cell carcinoma and adenocarcinoma. Eleven patients had a *de novo* presentation of small-cell carcinoma of the prostate (i.e., no known history of prior prostate adenocarcinoma).

Table 1. Baseline clinical characteristics

Patient characteristics	
Number of patients treated	60
Median age (years)	67 years (45–87)
Prior local therapy (surgery or radiation)	37 (61%)
Gleason grade	8
6	6 (13%)
7	15 (33%)
8–10	26 (59%)
Median PSA (ng/mL)	1.07 (0.01–514.2)
Sites of metastases	
Bone	47 (78%)
Lymph node	45 (75%)
Lung	22 (37%)
Liver	36 (60%)
Any visceral	41 (68%)
Elevated LDH	29/57 (51%)
Median number of prior systemic therapies for CRPC	3
Platinum	35 (58%)
Enzalutamide or abiraterone	24 (40%)
Docetaxel	19 (32%)
Cabazitaxel	6 (10%)
Radium-223	1 (2%)
Histologic diagnosis of NEPC by local review (inclusion criteria 1)	45 (75%)
Prostate adenocarcinoma plus ≥50% IHC staining for neuroendocrine markers (inclusion criteria 2)	11 (18%)
Development of liver metastases in the absence of PSA progression (inclusion criteria 3)	15 (25%)
Serum chromogranin >5× ULN and/or NSE>2× ULN (inclusion criteria 4)	18 (30%)
Median time from prostate cancer diagnosis to dose (months)	44.23 (3.9–1,313)

NOTE: A total of 75 patients were screened and 60 patients were treated.

The median duration of drug exposure was 7.0 weeks (IQR 5.3–14.1 weeks). For the primary endpoint, 8 patients (13.4%) were progression free at 6 months (16.7% NEPC; 5.3% CRPC-Adeno). Eighteen patients on study (30%) had stable disease or better at cycle 3 scans, all of whom had demonstrated progression prior to starting alisertib; the majority (89%) of them had NEPC histology (clinical features summarized in Supplementary Table S2). Overall median PFS was 2.2 months [95% confidence interval (CI), 2.0–2.6; 2.3 months, NEPC, 2.0 months, CRPC-Adeno; Fig. 1A; Supplementary Fig. S1] and objective response rate was 3.3%. Exceptional responders were identified (Supplementary Figs. S2–S5) and described below including 2 with complete resolution of liver metastases on therapy and 2 with prolonged stable disease (14 months and 3.8 years).

Median OS was 9.5 months (95% CI, 7.4–13.0) with no significant differences between NEPC and CRPC-Adeno (9.5 vs. 8.6 months, respectively, $P = 0.28$; Figs. 1B; Supplementary Fig. S1). Forty-eight deaths were recorded on-study, mostly because of progressive disease. Median OS of patients with lymph node and/or bone-only metastases was 12.1 months compared with 9.4 months for those with visceral metastases ($P = 0.08$).

Reasons for treatment discontinuation were disease progression (88%), AEs (8%), or unrelated medical condition (3%). The toxicity profile was as expected on the basis of prior trials of alisertib (Supplementary Tables S3 and S4) with most common AEs being fatigue (78%), anorexia (45%), and nausea (38%). Grade 3–4 neutropenia occurred in 13%, febrile neutropenia in 6.6%, and grade 3–4 thrombocytopenia in 5%. The most common grade ≥3 nonhematologic toxicities were fatigue (10%), GI (10%), and dehydration (5%). Dose reductions and/or delays were necessary in 37% patients. A similar proportion of patients with NEPC and CRPC-Adeno reported treatment-related AEs.

Molecular analyses

Forty-nine patients had pretreatment metastatic biopsies sufficient for WES, 20 for both WES and RNA-seq, and 25 for *AURKA* and *MYCN* FISH. Genomic analysis including purity and ploidy determined by CLONET (28), genomic burden, mutation rate, and differences between NEPC and CRPC-Adeno are shown in Fig. 2 and Supplementary Fig. S6. Recurrent mutations and somatic copy-number alterations included *RB1* deletion (55%), *TP53* mutation or deletion (46%), *PTEN* deletion (29%), and *BRCA2* mutation or deletion (29%). There was a lower frequency of *AR* amplification and mutations (29%) in this cohort compared with what has been reported in CRPC (29) and consistent with what we have previously reported in NEPC (4). As expected, expression of AR and AR signaling genes was lower in NEPC and

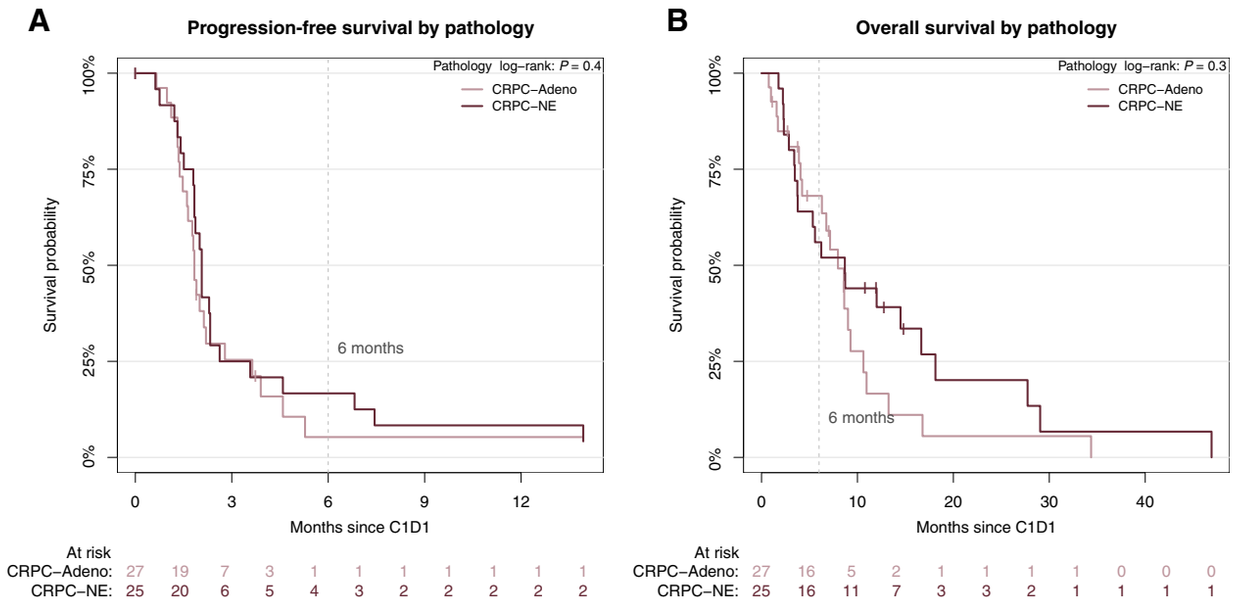

Figure 1.

Progression-free survival (**A**) and overall survival Kaplan–Meier curves (**B**) based on pathology subtype by central pathology review (CRPC-Adeno, red; NEPC, blue). PFS and OS for the entire cohort are shown in Supplementary Fig. S5.

expression of NEPC-associated genes was higher in NEPC, but there was a spectrum within both pathologic subgroups (Supplementary Fig. S7). Overall 24% of evaluable cases harbored *AURKA* or *MYCN* amplification (16% *AURKA*, 16% *MYCN*, and 8% concurrent), lower than observed in prior studies of treatment related NEPC (21). Aurora kinase A (*AURKA*) amplification was

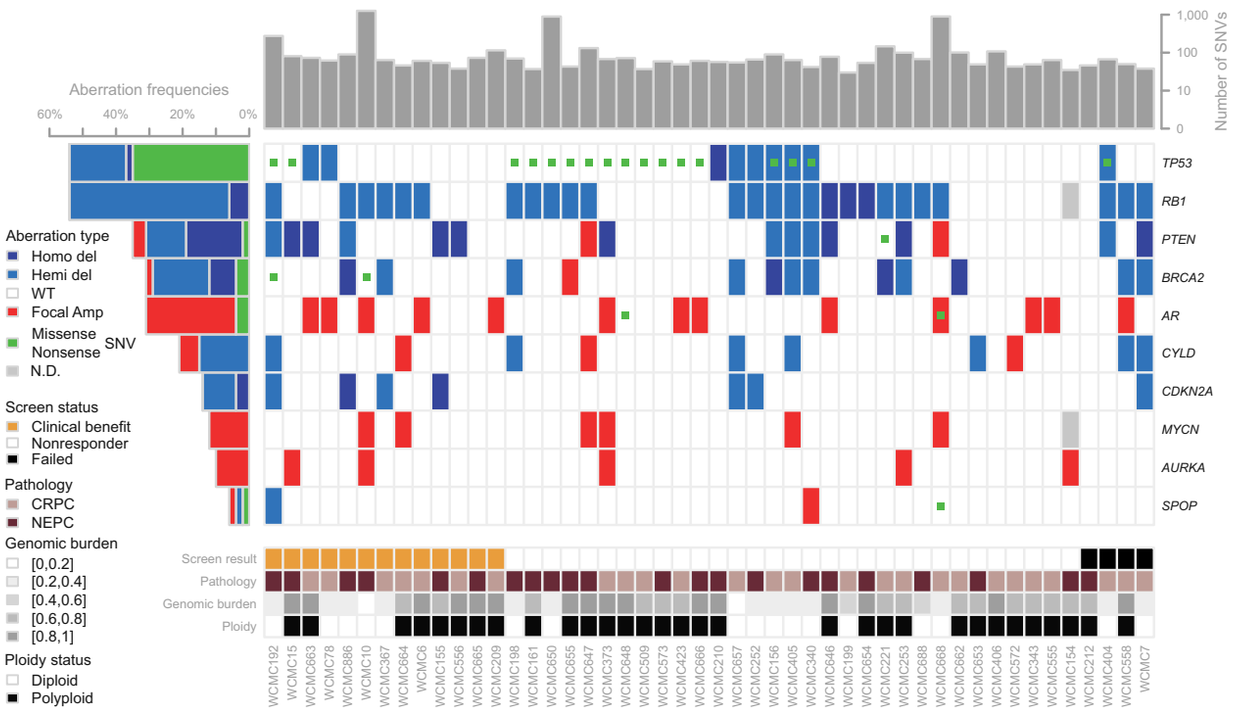

Figure 2.

WES analysis of the cohort annotated by pathology subtype (CRPC-Adeno, pink; NEPC, purple) using the same methodologies described by Beltran and colleagues (4). Plot shows total number of SNVs, aberrations in relevant genes, including nonsense and missense SNVs, copy-number deletions, and focal amplifications. Copy-number cells derive from $\log_2$ ratio (tumor/normal) adjusted by ploidy and tumor purity. Deletions and amplifications are defined using the thresholds on $\log_2$ ratio.

associated with improved OS ($P = 0.05$) but no difference in PFS ($P = 0.4$) on alisertib (Supplementary Fig. S8; log-rank test). While N-myc (*MYCN)* amplification was not associated with outcomes across the cohort, responders were identified that demonstrated molecular features suggestive of *MYCN* overactivity.

Patient 10 developed progressive bulky retroperitoneal and pelvic nodal (up to 7.5 cm) and new bone metastases within 6 months on primary androgen deprivation therapy (ADT) for metastatic prostate cancer, serum PSA 3 ng/mL, and chromogranin 1,379 ng/mL (upper limit, 95). Lymph node biopsy revealed neuroendocrine morphology with diffuse staining for chromogranin and synaptophysin (Supplementary Fig. S1). The patient was treated with alisertib, which he tolerated well and was maintained on therapy with no evidence of progression at 3.8 years. His tumor demonstrated hypermutated phenotype, mutation of *MSH6*, as well as concurrent genomic amplification of both *MYCN* and *AURKA* (Supplementary Fig. S1) possibly contributing to his long-term durable response.

Patient 886 initially presented with *de novo* small-cell carcinoma of the prostate with local invasion and extensive liver and lytic bone metastases, serum PSA 5.2 ng/mL. He was treated with carboplatin and etoposide without response (primary refractory) including progression in liver. He was started on alisertib and had complete resolution of metastases within 3 months (Supplementary Fig. S2). The patient was maintained on alisertib for 8.3 months in near CR. He subsequently developed parenchymal brain metastases without evidence of systemic relapse. His pretreatment liver biopsy had demonstrated small-cell carcinoma (Supplementary Fig. S2) with focal deletion of *CDKN2A*, *CDKN2B*, *RB1*, and *BRCA2*, low AR signaling, and elevated neuroendocrine markers (Supplementary Fig. S2). Although *AURKA* was not amplified and only 20% of tumor cells harbored *MYCN* amplification by FISH (Supplementary Fig. S2), there was significant *AURKA* and *MYCN* overexpression (Supplementary Fig. S3).

Patient 155 developed innumerable lung and liver metastases after 12 months of primary ADT for metastatic prostate cancer. Serum PSA was 0.2 ng/mL, chromogranin A was elevated at 1,157 ng/mL, NSE 61.2 ug/L, CEA 128 ng/mL. Liver biopsy revealed small-cell NEPC. He was treated with alisertib and within 12 weeks had improvement in symptoms and complete resolution of liver and lung metastases (Fig. 3A). His CEA and serum neuroendocrine markers rapidly normalized (Fig. 3B). Radiographic CR was maintained for 14 months. Therapy was then held for an intervening illness (gallstone cholecystitis); during this time, he developed rapid progression including brain metastases. WES of his pretreatment and progression tumor biopsies as well as pretreatment of circulating tumor DNA (ctDNA) showed high degree of genomic similarity between the 3 samples (Fig. 3C) suggesting minimal intrapatient tumoral heterogeneity in this patient. All 3 samples harbored focal loss of *PTEN and CDKN2A*. *AURKA* and *MYCN* were not amplified but were overexpressed. Large-scale deletions involving *FANCA*, *SMARCB1*, and *FBXW7* were identified. *FBXW7* encodes the Fbox protein that regulates degradation of both Aurora A and N-myc by targeting them for ubiquitization (16, 30). There was a similar clonality of mutations observed in his progression tumor, high NEPC score, and low AR signaling, suggesting that after therapeutic release from alisertib, the tumor retained its original molecular profile (Fig. 3D).

A patient-derived organoid was developed from the pretreatment biopsy of exceptional responder patient 155 and compared with another organoid (Fig. 4A) developed from a bone biopsy from another patient on this alisertib trial (patient 154), who presented with small-cell NEPC after prior ADT and platinum-etoposide with progressive bone, lung, and liver metastases; he did not respond to alisertib (progressed within 3 months). Both organoids were characterized histologically and molecularly (23), and were concordant with their matched patient tumor and AR negative by IHC (Fig. 4A). The organoids were treated with alisertib *in vitro* and demonstrated directionally similar responses as observed in the clinic by their corresponding patients (Fig. 4B; Supplementary Fig. S9). Alisertib consistently disrupted the N-myc–Aurora A complex in control cell lines (Fig. 4C; Supplementary Fig. S10; ref.14), but was not capable of disrupting their allosteric interaction in 154 organoids (the nonresponder patient) despite high baseline levels of N-myc–Aurora A. These data point to the potential utility of the N-myc–Aurora A proximal ligation assay as a functional readout of alisertib on-target effect and sensitivity.

Discussion

It has become increasingly recognized that a subset of advanced prostate tumors evolve to become less dependent on the AR (2–4). AR-independence is challenging to recognize clinically and neuroendocrine features may not always be present on tumor biopsy. Recent evidence suggests that NEPC arises clonally from prostate adenocarcinoma cells during the course of therapy through the acquisition of genomic and epigenomic alterations (4, 31), yet the clinical and molecular features, and timing of these events are not well defined. In this trial, we sought to address some of these challenges by establishing specific inclusion criteria to stratify the heterogeneously defined entity of NEPC from both a clinical and pathologic standpoint. While we did not expect all patients with clinical criteria to demonstrate pathologic features of NEPC, we posited that these aggressive tumors would share molecular features and therapy responsiveness with NEPC. The goal of establishing multiple inclusion cohorts was in line with Prostate Cancer Working Group 3 objectives to identify which patient features are most likely to benefit by any criteria (e.g., clinical, radiologic, and biologic) as a strategy to inform future trials (32).

Collectively, the trial enrolled patients with aggressive disease including those previously treated with platinum chemotherapy. Median PSA on this study was low at 1.13 ng/mL supportive of less AR-driven disease. We learned that the genomic profiles, range of AR signaling, and expression of neuroendocrine markers varied, which may reflect limitations of single site biopsy and/or a biologic spectrum of CRPC, with initial retention of the AR and expression of luminal prostate markers even in tumors that start to lose AR dependence (5, 6, 14). Although the study did not meet its primary endpoint, significant responders were identified with molecular alterations potentially contributing to response. The overall lack of strong signal of alisertib response across the cohort may reflect challenges of underlying heterogeneity, context with other drivers of CRPC, and/or the mechanism of action of alisertib that may not be inhibiting N-myc sufficiently.

Responders on the study included those with extensive visceral metastases and platinum-refractory disease. Notably, one of the

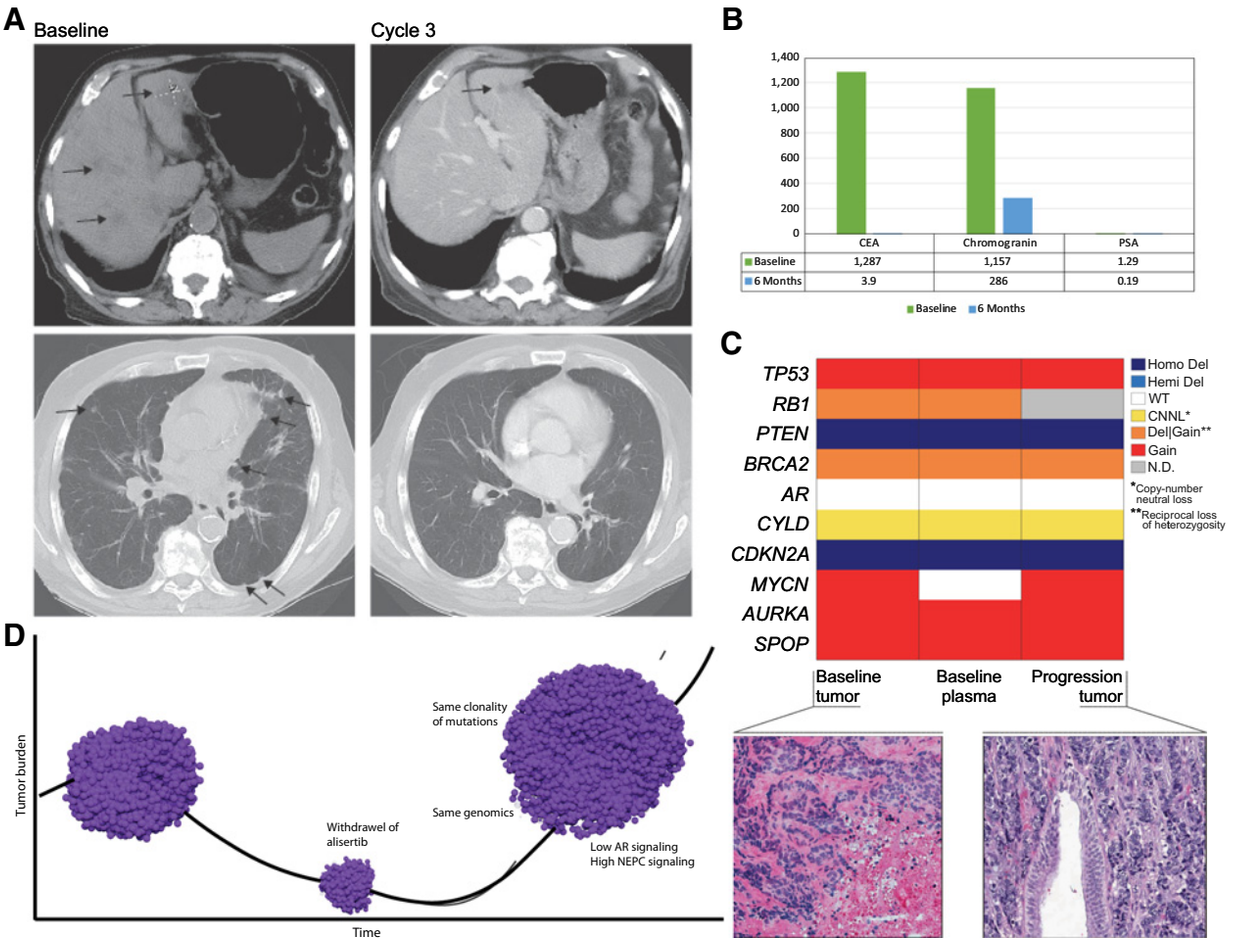

Figure 3.

A, Exceptional responder patient 155 CT scan at baseline (pretreatment) and after cycle 3. **B,** Serum chromogranin, CEA, and PSA at baseline and after 6 months on alisertib. **C,** Comparison of copy number of representative genes (determined by WES) showing concordance between baseline biopsy, baseline ctDNA, and progression biopsy; colors represent allele-specific copy-number states; hematoxylin and eosin (H&E) images showing pretreatment baseline tumor biopsy and posttreated (progression) tumor both showing similar morphology (small-cell carcinoma). **D,** Schematic of patient 155 tumor response and progression after therapeutic release from alisertib (drug was held 17 days). Pretreatment biopsy, AR signaling score 0.04; NEPC score 0.5; progression tumor, AR signaling score 0.05; NEPC score 0.47.

highlighted exceptional responders to alisertib had a *de novo* presentation of small-cell prostate cancer with a clinical presentation of visceral and lytic bone metastases. These data suggest that there may be similarities between this subgroup and the more common treatment-related NEPC, and further study of the role of N-myc and Aurora A in *de novo* small-cell prostate cancer is warranted. Alisertib has also been investigated in other *de novo* neuroendocrine tumors including small-cell lung cancer and neuroblastoma with the cooperation of Aurora A and Myc family transcription factors (8).

The results from exceptional responder patient 155 highlight the impact of intrapatient tumor consistency (or lack of heterogeneity) in mediating therapeutic response to a targeted therapy. The considerable similarity of the WES of pretreatment and progression biopsies and ctDNA suggests shared vulnerabilities across tumor metastases potentially contributing toward the patient's dramatic clinical response. Upon release of the therapeutic pressure of alisertib, the patient developed rapid progression, with tumor transcriptome changes associated with NEPC progression and a maintained genomic profile, suggesting that that the patient may have responded to retreatment had he been well enough to do so.

Given the heterogeneity within this clinically enriched trial subgroup, future trials for non-AR–driven disease should be aimed at molecularly defined inclusion criteria. This is especially important as distinct subclasses of prostate cancer are biologically characterized, including not only NEPC but also other AR-independent subtypes such as double-negative (AR-negative, NE-negative) CRPC (2). Understanding the spectrum and chronology of the molecular events underlying disease progression will allow us to identify patient subsets on the basis of their underlying resistance patterns and will pave the way for noninvasive testing (e.g., ctDNA or circulating tumor cell profiles), as metastatic biopsies are invasive and remain challenging to perform serially in patients.

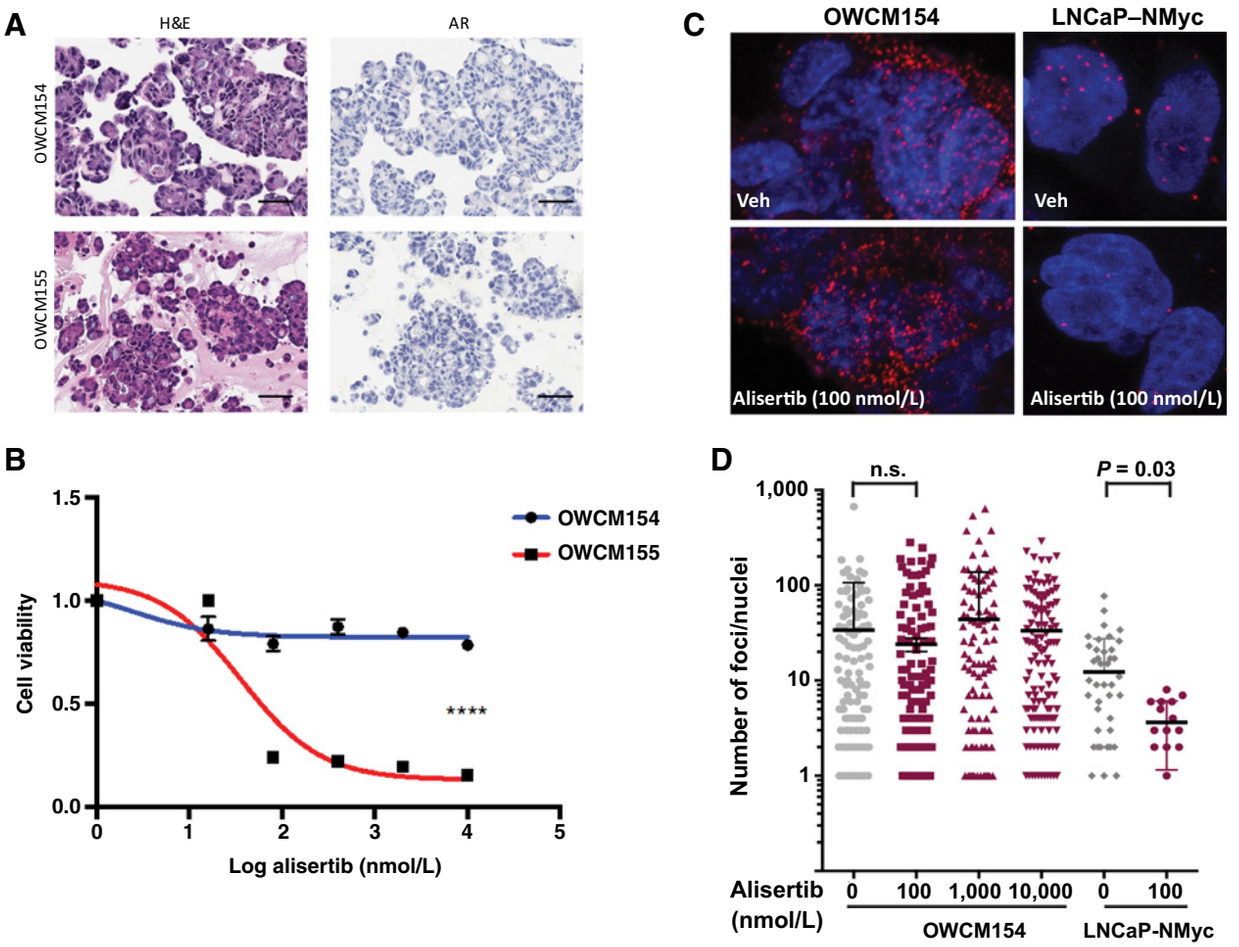

Figure 4.

A, Representative H&E images of tumor organoids derived from pretreatment biopsies of patients 154 (liver) and 155 (bone) both showing small-cell carcinoma, AR-negative by IHC. **B,** Cell viability graph using NEPC patient-derived organoids. A significant effect of alisertib is observed in OWCM155 (red; IC_{50} = 35.98 nmol/L), $P < 0.0001$, **** compared with the resistant NEPC organoid OWCM154 (blue). Organoids were treated with increasing doses of alisertib (range 16 nmol/L–10 μmol/L) for 6 days and viability was determined using CellTiter Glo (Promega). Statistical analysis was performed on 3 independent biological replicates using a nonlinear regression curve fit (3 parameters) method in Prism 6 for Mac Os X. **C,** Proximal ligation assay (PLA) to measure the interaction between N-myc and Aurora A and quantify the amount of complex present in organoids using *in situ* probes (14). Shown here are representative confocal images of the N-Myc/Aurora A complex PLA visualized by discreet red dots in OWCM154 and LNCaP–N-Myc cells treated with 100 nmol/L of alisertib or vehicle for 24 hours or 72 hours, respectively (top). Fixed cells were incubated with antibodies against N-Myc [dilution, 1/200; sc53993 (B8.4.B, N-Myc) and Aurora-A (dilution, 1/200; Cell Signaling Technology 4718S], and interactions were revealed using secondary antibodies coupled to PLA DNA probes that hybridized and enzymatically joined when in close proximity. After rolling circle amplification, each interaction generated a fluorescent spot. **D,** Confocal microscopy quantifications were carried out using BlobFinder software (33) using minimum nucleus size: 50 pixel^2; blob threshold, 12. Shown is a summary of the quantification of number of PLA dots calculated from OWCM154 and cells (number of nuclei evaluation per dose: $n = 115$, 0 nmol/L; $n = 164$, 100 nmol/L; $n = 135$, 1,000 nmol/L; and $n = 137$; 10,000 μmol/L) or LNCaP-NMyc cells (number of nuclei evaluation per dose: $n = 49$, 0 nmol/L and $n = 16$, 100 nmol/L).

The development of patient-derived organoids from patients on early-phase clinical trials represents a unique approach for patient interrogation. We have demonstrated how organoid models maintain the genomic profiles of their corresponding tumor biopsies (23) and here show how they recapitulate the drug responses of the patients, and therefore may be useful tools as patient "avatars" for coclinical trials and as a resource to inform drug and biomarker development. In prostate cancer, this is especially relevant as there are few cell line models and only one bona fide NEPC cell line (the NCI-H660 cell line) widely available for preclinical studies. Such models may be used to study dynamic biomarkers to evaluate pharmacodynamic effects of drug such as the PLA assay described in this study, which could be applicable for future preclinical studies and trials using alisertib or other inhibitors of the AURKA–MYCN complex.

Cancers may adopt different means to evade therapy and evolve in the face of pressure from a targeted therapy. Further investigation of targeting N-myc and the Aurora A–N-myc complex for patients with AR-independent NEPC is warranted but biomarker selection will be critical.

Disclosure of Potential Conflicts of Interest

H. Beltran reports receiving commercial research grants from Millenium Pharmaceuticals. M. Stein reports receiving commercial research grants from Oncoceutics, Merck Sharpe Dohme, Janssen Oncology, and Advaxis, and is a consultant/advisory board member for Merck Sharpe Dohme. H.I. Scher reports receiving commercial research grants from Janssen and is a consultant/advisory board member for Janssen Research Development. D.M. Nanus is a consultant/advisory board member for Roche Genentech. K.V. Ballman reports receiving other remuneration from Janssen. No potential conflicts of interest were disclosed by the other authors.

Authors' Contributions

Conception and design: H. Beltran, M.A. Rubin, H.I. Scher, D.M. Nanus, S.T. Tagawa
Development of methodology: H. Beltran, B. Montgomery, C. Hoimes, J.M. Mosquera, E. Dardenne, M.A. Rubin, H.I. Scher, D.S. Rickman, S.T. Tagawa
Acquisition of data (provided animals, acquired and managed patients, provided facilities, etc.): H. Beltran, D.C. Danila, B. Montgomery, C. Hoimes, R.Z. Szmulewitz, U. Vaishampayan, A.J. Armstrong, M.Stein, J. Pinski, J.M. Mosquera, V. Sailer, N. Gumpeni, E. Dardenne, L. Puca, H.I. Scher, D.S. Rickman, D.M. Nanus, S.T. Tagawa
Analysis and interpretation of data (e.g., statistical analysis, biostatistics, computational analysis): H. Beltran, C. Oromendia, D.C. Danila, B. Montgomery, C. Hoimes, U. Vaishampayan, A.J. Armstrong, M.Stein, J.M. Mosquera, V. Sailer, R. Bareja, A. Romanel, A. Sboner, E. Dardenne, L. Puca, D. Prandi, M.A. Rubin, F. Demichelis, D.M. Nanus, K.V. Ballman, S.T. Tagawa
Writing, review, and/or revision of the manuscript: H. Beltran, C. Oromendia, D.C. Danila, B. Montgomery, C. Hoimes, R.Z. Szmulewitz, U. Vaishampayan, A.J. Armstrong, M. Stein, J.M. Mosquera, V. Sailer, A. Sboner, M.A. Rubin, H.I. Scher, F. Demichelis, D.M. Nanus, K.V. Ballman, S.T. Tagawa
Administrative, technical, or material support (i.e., reporting or organizing data, constructing databases): H. Beltran, C. Oromendia, V. Sailer, L. Puca
Study supervision: H. Beltran, U. Vaishampayan, A.J. Armstrong, S.T. Tagawa

Acknowledgments

We are grateful to our patients and their families for participation in this study. We appreciate all the work of the site coordinators, data managers, and investigators. In particular, we would like to acknowledge Irene Karpenko, Gillian Hodes, Olivera Calukovic, Michael Sigouros, Danielle Pancirer, Jessica Padilla, Theresa MacDonald, and Terra McNary for their help with regulatory, tissue, and data coordination for this study. This work was supported by Millennium Pharmaceuticals, Inc and the Prostate Cancer Foundation. Additional funding sources include the Department of Defense PC131961 (to D.M. Nanus, S.T. Tagawa, and H. Beltran), PC121341 (to H. Beltran), PC160264 (to H. Beltran and D.S. Rickman), PC121111 (to H.I. Scher), and PC131984 (to H.I. Scher); NIH/NCI SPORE in Prostate Cancer P50-CA211024 (to H. Beltran, J.M. Mosquera, M.A. Rubin, and D.S. Rickman) and P50-CA92629 (to H.I. Scher); NIH/NCI Cancer Center Support Grant P30-CA008748 (to H.I. Scher); and the Ann and William Bresnan Foundation (to H. Beltran and D.M. Nanus).

The costs of publication of this article were defrayed in part by the payment of page charges. This article must therefore be hereby marked *advertisement* in accordance with 18 U.S.C. Section 1734 solely to indicate this fact.

Received June 18, 2018; revised August 12, 2018; accepted September 14, 2018; published first September 19, 2018.

References

1. Watson PA, Arora VK, Sawyers CL. Emerging mechanisms of resistance to androgen receptor inhibitors in prostate cancer. Nat Rev Cancer 2015;15:701–11.
2. Bluemn EG, Coleman IM, Lucas JM, Coleman RT, Hernandez-Lopez S, Tharakan R, et al. Androgen receptor pathway-independent prostate cancer is sustained through FGF signaling. Cancer Cell 2017;32:474–89.
3. Aggarwal R, Huang J, Alumkal JJ, Zhang L, Feng FY, Thomas GV, et al. Clinical and genomic characterization of treatment-emergent small-cell neuroendocrine prostate cancer: a multi-institutional prospective study. J Clin Oncol 2018;36:2492–2503.
4. Beltran H, Prandi D, Mosquera JM, Benelli M, Puca L, Cyrta J, et al. Divergent clonal evolution of castration-resistant neuroendocrine prostate cancer. Nat Med 2016;22:298–305.
5. Mu P, Zhang Z, Benelli M, Karthaus WR, Hoover E, Chen CC, et al. SOX2 promotes lineage plasticity and antiandrogen resistance in TP53- and RB1-deficient prostate cancer. Science 2017;355:84–8.
6. Ku SY, Rosario S, Wang Y, Mu P, Seshadri M, Goodrich ZW, et al. Rb1 and Trp53 cooperate to suppress prostate cancer lineage plasticity, metastasis, and antiandrogen resistance. Science 2017;355:78–83.
7. Beltran H, Tagawa ST, Park K, MacDonald T, Milowsky MI, Mosquera JM, et al. Challenges in recognizing treatment-related neuroendocrine prostate cancer. J Clin Oncol 2012;30:e386–9.
8. Rickman DS, Beltran H, Demichelis F, Rubin MA. Biology and evolution of poorly differentiated neuroendocrine tumors. Nat Med 2017;23:1–10.
9. Aparicio AM, Harzstark AL, Corn PG, Wen S, Araujo JC, Tu SM, et al. Platinum-based chemotherapy for variant castrate-resistant prostate cancer. Clin Cancer Res 2013;19:3621–30.
10. Aparicio AM, Shen L, Tapia EL, Lu JF, Chen HC, Zhang J, et al. Combined tumor suppressor defects characterize clinically defined aggressive variant prostate cancers. Clin Cancer Res 2016;22:1520–30.
11. Beltran H, Tomlins S, Aparicio A, Arora V, Rickman D, Ayala G, et al. Aggressive variants of castration-resistant prostate cancer. Clin Cancer Res 2014;20:2846–50.
12. Wang HT, Yao YH, Li BG, Tang Y, Chang JW, Zhang J. Neuroendocrine Prostate Cancer (NEPC) progressing from conventional prostatic adenocarcinoma: factors associated with time to development of NEPC and survival from NEPC diagnosis-a systematic review and pooled analysis. J Clin Oncol 2014;32:3383–90.
13. Beltran H, Rickman DS, Park K, Chae SS, Sboner A, MacDonald TY, et al. Molecular characterization of neuroendocrine prostate cancer and identification of new drug targets. Cancer Discov 2011;1:487–95.
14. Dardenne E, Beltran H, Benelli M, Gayvert K, Berger A, Puca L, et al. N-Myc induces an EZH2-mediated transcriptional program driving neuroendocrine prostate cancer. Cancer Cell 2016;30:563–77.
15. Lee JK, Phillips JW, Smith BA, Park JW, Stoyanova T, McCaffrey EF, et al. N-Myc drives neuroendocrine prostate cancer initiated from human prostate epithelial cells. Cancer Cell 2016;29:536–47.
16. Otto T, Horn S, Brockmann M, Eilers U, Schüttrumpf L, Popov N, et al. Stabilization of N-Myc is a critical function of Aurora A in human neuroblastoma. Cancer Cell 2009;15:67–78.
17. Brockmann M, Poon E, Berry T, Carstensen A, Deubzer HE, Rycak L, et al. Small molecule inhibitors of aurora-a induce proteasomal degradation of N-myc in childhood neuroblastoma. Cancer Cell 2013;24:75–89.
18. Scher HI, Halabi S, Tannock I, Morris M, Sternberg CN, Carducci MA, et al. Design and end points of clinical trials for patients with progressive prostate cancer and castrate levels of testosterone: recommendations of the Prostate Cancer Clinical Trials Working Group. J Clin Oncol 2008;26:1148–59.
19. Magi A, Tattini L, Cifola I, D'Aurizio R, Benelli M, Mangano E, et al. EXCAVATOR: detecting copy number variants from whole-exome sequencing data. Genome Biol 2013;14:R120.
20. Beltran H, Wyatt AW, Chedgy EC, Donoghue A, Annala M, Warner EW, et al. Impact of therapy on genomics and transcriptomics in high-risk prostate cancer treated with neoadjuvant docetaxel and androgen deprivation therapy. Clin Cancer Res 2017;23:6802–11.
21. Mosquera JM, Beltran H, Park K, MacDonald TY, Robinson BD, Tagawa ST, et al. Concurrent AURKA and MYCN gene amplifications are harbingers of lethal treatment-related neuroendocrine prostate cancer. Neoplasia 2013;15:1–10.
22. Gao D, Vela I, Sboner A, Iaquinta PJ, Karthaus WR, Gopalan A, et al. Organoid cultures derived from patients with advanced prostate cancer. Cell 2014;159:176–87.
23. Puca L, Bareja R, Prandi D, Shaw R, Benelli M, Karthaus WR, et al. Patient derived organoids to model rare prostate cancer phenotypes. Nat Commun 2018;9:2404.

24. Meulenbeld HJ, Bleuse JP, Vinci EM, Raymond E, Vitali G, Santoro A, et al. Randomized phase II study of danusertib in patients with metastatic castration-resistant prostate cancer after docetaxel failure. BJU Int 2013;111:44–52.
25. Rathkopf DE, Antonarakis ES, Shore ND, Tutrone RF, Alumkal JJ, Ryan CJ, et al. Safety and antitumor activity of apalutamide (ARN-509) in metastatic castration-resistant prostate cancer with and without prior abiraterone acetate and prednisone. Clin Cancer Res 2017;23:3544–51.
26. A'Hern RP. Sample size tables for exact single-stage phase II designs. Stat Med 2001;20:859–66.
27. Epstein JI, Amin MB, Beltran H, Lotan TL, Mosquera JM, Reuter VE, et al. Proposed morphologic classification of prostate cancer with neuroendocrine differentiation. Am J Surg Pathol 2014;38:756–67.
28. Prandi D, Baca SC, Romanel A, Barbieri CE, Mosquera JM, Fontugne J, et al. Unraveling the clonal hierarchy of somatic genomic aberrations. Genome Biol 2014;15:439.
29. Robinson D, Van Allen EM, Wu YM, Schultz N, Lonigro RJ, Mosquera JM, et al. Integrative clinical genomics of advanced prostate cancer. Cell 2015;161:1215–28.
30. Kwon YW, Kim IJ, Wu D, Lu J, Stock WA, Liu Y, et al. Pten regulates Aurora-A and cooperates with Fbxw7 in modulating radiation-induced tumor development. Mol Cancer Res 2012;10:834–44.
31. Zou M, Toivanen R, Mitrofanova A, Floch N, Hayati S, Sun Y, et al. Transdifferentiation as a mechanism of treatment resistance in a mouse model of castration-resistant prostate cancer. Cancer Discov 2017;7:736–49.
32. Scher HI, Morris MJ, Stadler WM, Higano C, Basch E, Fizazi K, et al. Trial design and objectives for castration-resistant prostate cancer: updated recommendations from the Prostate Cancer Clinical Trials Working Group 3. J Clin Oncol 2016;34:1402–18.
33. Allalou A, Wählby C. BlobFinder, a tool for fluorescence microscopy image cytometry. Comput Methods Programs Biomed 2009;94:58–65.